

Barbara, Calif., 4-15 August 1969 (unpublished), and references therein.

³G. M. Comstock, C. Y. Fan, and J. A. Simpson, *Astrophys. J.* **146**, 51 (1966).

⁴C. E. McIlwain, *J. Geophys. Res.* **66**, 3681 (1961).

⁵L. J. Lanzerotti, *Phys. Rev. Lett.* **21**, 929 (1968).

⁶Only oxygen ions have been measured so far in the plasmasphere: K. K. Harris, G. W. Sharp, and C. R.

Chappell, *J. Geophys. Res.* **75**, 219 (1970).

⁷G. Pizzella, Univ. of Iowa Report No. 70-9, 1970 (to be published).

⁸J. J. Bame, A. J. Hundhausen, J. R. Asbridge, and I. B. Strong, *Phys. Rev. Lett.* **20**, 393 (1968).

⁹M. P. Nakada and G. D. Mead, *J. Geophys. Res.* **70**, 4777 (1965).

¹⁰B. A. Tverskoy, *Geomagn. Aeron.* **5**, 617 (1965).

Evidence for the Existence of a New Meson in the 955-MeV Mass Region*

M. Aguilar-Benitez, D. Bassano, R. L. Eisner, J. B. Kinson, D. Pandoulas, and N. P. Samios
Brookhaven National Laboratory, Upton, New York 11973

and

V. E. Barnes

Brookhaven National Laboratory, Upton, New York 11973, and Purdue University, Lafayette, Indiana 47907

(Received 15 September 1970)

We report evidence for the existence of a new meson, which we call the $M(953)$, with mass 953 ± 2 MeV and width <10 MeV, produced in the final state $K^-p \rightarrow pK^-M^0$ at incident momenta 3.9 and 4.6 GeV/c. These results are based primarily on a signal of 68 ± 12 events in the decay mode $M \rightarrow \pi^+\pi^-\gamma$ where the $\pi\pi$ system does not show a ρ^0 signal, in sharp distinction to the $\rho^0\gamma$ decay mode of the $\eta'(958)$.

The 960-MeV mass region for nonstrange mesons is remarkable for the variety of effects already reported, most notably the $\eta'(958)$ meson¹ of very narrow decay width which is believed to complete the nonet of $J^P = 0^-$ mesons, the $\delta(962)$ meson² reported from missing-mass spectrometer and bubble chamber studies, and the notorious $H(990)$ meson.³ We wish to report, in addition to the observation of the $\eta'(958)$, detection of a new nonstrange meson, which we call the $M(953)$, decaying into $\eta\pi^+\pi^-$ and into $\pi^+\pi^-\gamma$, where the $\pi^+\pi^-$ system does not show a ρ^0 . This is in contradistinction to the 100% $\rho^0\gamma$ content of the $\pi^+\pi^-\gamma$ decay of the $\eta'(958)$ seen both in our data and in the world data.⁴ The mass found for the M is 953 ± 2 MeV and the intrinsic width is $\Gamma < 10$ MeV (95% confidence level), which are consistent with the compiled values for the $\eta'(958)$. The $\pi^+\pi^-\gamma/\pi^+\pi^-\eta_N^0$ (where η_N^0 signifies decay to all neutrals) branching ratio of the $M(953)$ is found to be 1.2 ± 0.3 . We cannot associate the $M(953)$ with any known effect.

The data for this study come from exposures of the Brookhaven National Laboratory (BNL) 80-in. hydrogen bubble chamber to beams of K^- mesons at 3.9- and 4.6-GeV/c incident momenta. The final states of interest are (1) $pK^-\pi^+\pi^-$, (2) $pK^-\pi^+\pi^-\pi^0$, (3) $pK^-\pi^+\pi^-\pi^0$, (4) $pK^-\pi^+\pi^-\eta_N^0$, (5) $\Lambda\pi^+\pi^-$, (6) $\Lambda\pi^+\pi^-\gamma$, (7) $\Lambda\pi^+\pi^-\pi^0$, and (8) $\Lambda\pi^+\pi^-\eta_N^0$. Events

were assigned to the four-constraint (4C) categories (1) and (5) if the χ^2 probability was greater than 1% and ionization, as measured by the BNL flying-spot digitizer (FSD), was consistent with the kinematic interpretation. For Reactions (3) and (7), a 5% probability cut was normally imposed. Reactions (2) and (6) were not originally fitted, but are in fact found in the samples of Reactions (3) and (7). Therefore, in order not to lose γ events, we have retained all 1 C π^0 fits with probability greater than 0.1% which are consistent with ionization.

In Fig. 1(a) we show the unfitted⁵ $\pi^+\pi^-\pi^0$ effective mass from Reaction (3) for $\cos\theta^* > 0.0$.⁶ In order to favor γ events, the missing mass squared has been restricted to $MM^2 \leq 0.01$ GeV², where MM is defined as the mass recoiling against the seen particles, i.e., the mass of the " π^0 ." In addition to the ω signal, coming from the tail of the π^0 distribution, a sharp peak at a mass of about 955 MeV is seen consisting of 70 ± 14 events above background. The same mass spectrum, but for events with $MM^2 > 0.01$ GeV² (not shown), displays no evidence of structure in the 955-MeV mass region, indicating that the peak seen in Fig. 1(a) is not due to the tail of the π^0 . An investigation of alternative hypotheses has shown that the peak cannot be due to contamination from any other channel. In addition, there

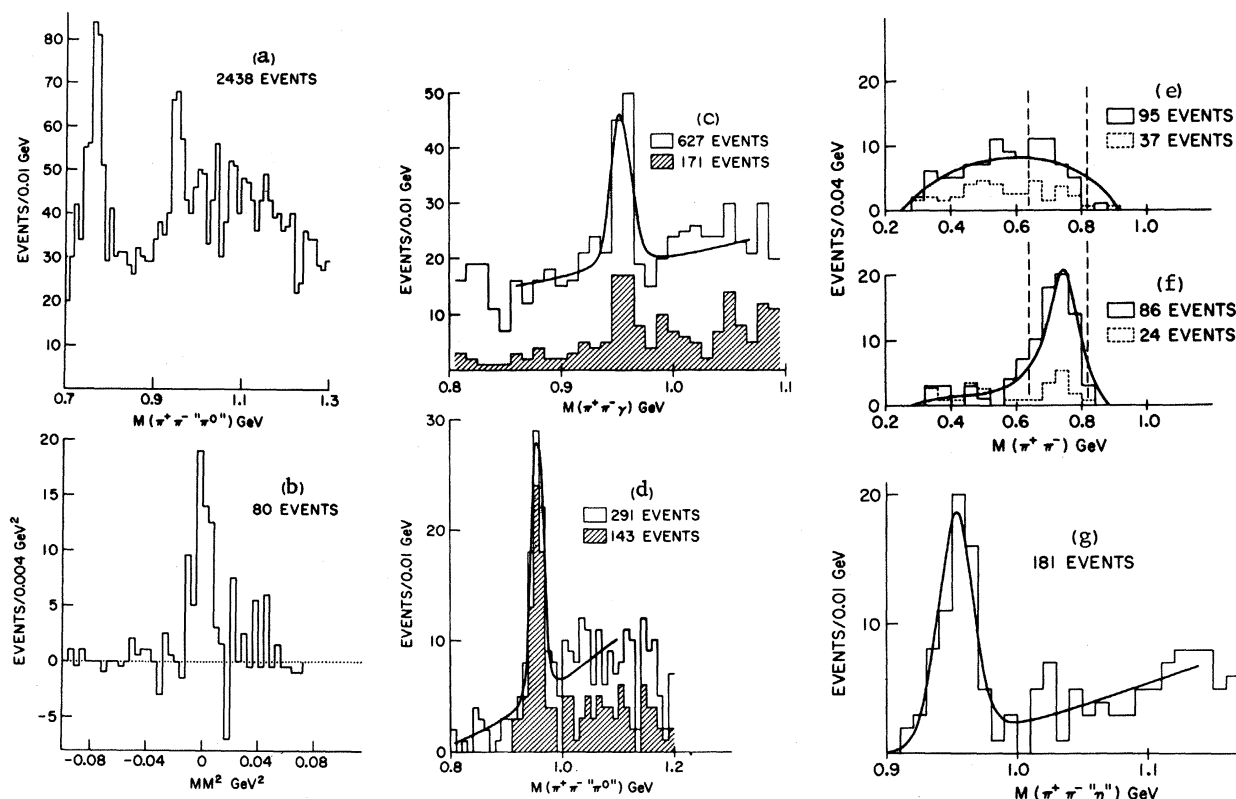


FIG. 1. (a) Unfitted $\pi^+\pi^-\pi^0$ effective mass spectrum for events that fit Reaction (3) with $\cos\theta^* > 0.0$ and $MM^2 < 0.01 \text{ GeV}^2$. (b) Background-subtracted spectrum of missing mass squared for the 0.940–0.970 GeV region. (c) $\pi^+\pi^-\gamma$ effective-mass spectrum for events that fit Reaction (2). The shaded histogram is the same mass spectrum with $M(\pi^+\pi^-)$ required to be in the ρ^0 region. (d) Unfitted $\pi^+\pi^-\pi^0$ effective-mass spectrum for events that fit Reaction (7) with $\cos\theta^* > 0.8$ and $MM^2 < 0.01 \text{ GeV}^2$. The shaded histogram is for events with $\pi^+\pi^-$ effective mass in the ρ^0 region. (e), (f) $\pi^+\pi^-$ mass projections for events in the M and η' regions, respectively. The dotted curves represent the $\pi^+\pi^-$ mass projections of the adjacent control bands normalized to the total number of events in the backgrounds under the resonances. The solid curves are the result of the fits described in the text. (g) $\eta_N^0\pi^+\pi^-$ effective mass spectrum for events that fit Reaction (4) with $\cos\theta^* > 0.0$.

is no evidence for any loss of γ events into reactions $K^-p \rightarrow K^-\pi^-\pi^+pMM$ and $K^-p \rightarrow K^-\pi^-\pi^+p$. To demonstrate that events in the signal in fact contain a γ , we plot the MM^2 spectrum [Fig. 1(b)] for events in the 955-MeV peak region minus events from control bands on either side, chosen to have an area equal to the estimated background in the peak region. A clear γ signal is seen, peaked at $MM^2 = 0$ and mainly lying below 0.01 GeV^2 . This separation is due to the high accuracy and precision afforded by the BNL FSD. There is no evidence for any residual π^0 's at $MM^2 = 0.018 \text{ GeV}^2$. To sharpen the mass resolution of the $\pi^+\pi^-\gamma$ system, we refitted all events of Fig. 1(a) having a $\pi^+\pi^-\pi^0$ effective mass between 0.8 and 1.1 GeV, adding to our normal kinematics hypotheses the $1C \gamma$ hypothesis of Reaction (2). We then repeated our fit-selection procedure using ionization estimates and kinematic-fit χ^2 probabilities. In Fig. 1(c) we plot the fitted $\pi^+\pi^-\gamma$ mass spectrum for

only those events with Reaction (2) as the best⁷ hypothesis and also kinematic χ^2 probability $> 5\%$. The peak at 955 MeV persists and becomes narrower, strengthening our belief that it is a genuine resonance and that it decays into $\pi^+\pi^-\gamma$. The curve shown is a maximum-likelihood fit using a Breit-Wigner shape with folded resolution⁸ plus a second order polynomial background shape and yields a mass of $953 \pm 2 \text{ MeV}$ and an intrinsic width of $< 10 \text{ MeV}$.⁹ The statistical significance of the peak is more than 5 standard deviations, corresponding to an excess of 68 ± 12 events. The shaded histogram of Fig. 1(c) shows the mass spectrum of the $\rho^0\gamma$ system where the ρ^0 is defined by $0.64 \leq M(\pi^+\pi^-) \leq 0.82 \text{ GeV}$. The number of events in the peak at 955 MeV is much reduced. Those remaining are in proportion to the $\frac{1}{3}$ of the $\pi^+\pi^-$ phase space included in the ρ^0 mass slice. This is incompatible with the branching ratio of the $\eta'(958)$ into $(\rho^0\gamma)/(\text{all } \pi^+\pi^-\gamma) = 1.0$

found in the world data, indicating that we are observing a new resonance which we call the $M(953)$.

Before returning to a quantitative demonstration of the above, we will first proceed to discuss the properties of the $\eta'(958)$ as observed in Reactions (6)-(8). For events which fit Reaction (7) with χ^2 probability greater than 0.1%, we plot in Fig. 1(d) the unfitted $\pi^+\pi^-\pi^0$ mass spectrum for events with $MM^2 \leq 0.01 \text{ GeV}^2$, to favor Reaction (6) and to eliminate most π^0 events.¹⁰ A very forward cut, $\cos\theta^*(p, \Lambda) > 0.8$, is imposed in view of the remarkably peripheral production¹¹ of η' in $K^-p \rightarrow \Lambda\eta'$ at these energies. A clear signal is seen between 0.93 and 0.98 GeV. A maximum-likelihood fit using a Gaussian plus a polynomial background shape gives a mass of $956 \pm 2 \text{ MeV}$ and a width consistent with our mass resolution of 20 MeV full width at half-maximum. The shaded histogram of Fig. 1(d) contains events in the ρ^0 slice as defined above, and we see that essentially all of the signal remains. Inspection of the background-subtracted MM^2 spectrum (not shown) from the mass region 0.93-0.98 GeV shows a clear peak at $MM^2 = 0$, strongly supporting a decay into $\rho\gamma$. The mass, width, and $\rho^0\gamma$ decay mode identify this enhancement as the $\eta'(958)$; we note its distinctive difference from the non- $\rho^0\gamma$ enhancement of Fig. 1(c).

A quantitative demonstration of the essential difference between the M and the η' is provided in Figs. 1(e) and 1(f), where the $\pi^+\pi^-$ mass projections of the M [Reaction (2)] and η' [Reaction (6)] regions are shown. The dotted histograms are suitably adjusted $\pi^+\pi^-$ mass projections from control regions below and above the resonance regions.¹² Clearly, the $\pi^+\pi^-$ mass distribution for the η' shows a large ρ^0 signal, while the corresponding distribution for the M is like phase space [solid curve in Fig. 1(e)]. A maximum-likelihood fit to the Dalitz plot for events in the η' region, using phase space plus a ρ Breit-Wigner modified by a matrix element¹³ corresponding to the decay of a $J^{PC} = 0^{-+}$ particle into $\rho^0\gamma$, gives $64 \pm 9 \rho^0$ events. As shown by the solid curve in Fig. 1(f), a good fit is obtained, with the $\pi^+\pi^-$ mass peaking at 730 MeV as do the data. The fit to Fig. 1(d) gives $63 \pm 9 \eta'$ events above background in the mass region 0.93 to 0.98 GeV. Moreover, outside the η' region, the $\pi^+\pi^-$ projection shows little ρ^0 (5 events), and we attribute $59 \pm 10 \rho^0$'s to the η' events. The resulting ratio $(\eta' \rightarrow \rho^0\gamma)/(\eta' \rightarrow \text{all } \pi^+\pi^-\gamma) = 0.94 \pm 0.20$, in excellent agreement with the world data. Performing a Dalitz-plot fit with the same matrix element for

the events in the M region, we obtain $3 \pm 6 \rho^0$ events from the 58 ± 10 resonance events. The ratio $(M \rightarrow \rho^0\gamma)/(M \rightarrow \text{all } \pi^+\pi^-\gamma) = 0.05 \pm 0.10$, and is in disagreement with our determination of the η' ratio by about 3.5 standard deviations.¹⁴ The inclusion of the world η' data strengthens this conclusion. This difference comprises the main evidence for the existence of yet another new boson resonance with mass in the 955-MeV region.

We now address ourselves to the question of an $\eta\pi\pi$ decay mode of the M . We show in Fig. 1(g) the $\pi^+\pi^-\eta_N^0$ effective mass spectrum of Reaction (4) with $\cos\theta^* > 0.0$. The η_N^0 is defined by the selection $0.27 \leq MM^2 \leq 0.33 \text{ GeV}^2$. A clear $\pi^+\pi^-\eta_N^0$ signal is seen in the 955-MeV mass region. We cannot attribute this peak to the $\pi^+\pi^-\eta'$ because any $\eta' \rightarrow \pi^+\pi^-\eta_N^0$ in Reaction (4) would imply an approximately equal amount of $\eta' \rightarrow \rho^0\gamma$ in Reaction (2), which is not observed. Fitting a Breit-Wigner with resolution folded in plus a polynomial background we obtain 58 ± 7 events above background, a mass of $951 \pm 4 \text{ MeV}$, and a width of $< 15 \text{ MeV}$ ⁹ (95% confidence level). The mass and width agree well with those of the $\pi\pi\gamma$ decay mode of the $M(953)$. On the assumption that the two decays are from the same object,¹⁵ the $\pi^+\pi^-\gamma/\pi^+\pi^-\eta_N^0$ branching ratio of the M is 1.2 ± 0.3 , similar to that obtained for the η' .

We cannot associate the $M(953)$ with any of the previously reported^{2,3} mesons in the 960 MeV region. In particular, we can rule out its being the $H(990)$ since we do not observe a $\pi^+\pi^-\pi^0$ decay mode. No evidence is found for the M decaying into $\pi^0\eta_N^0$,¹⁶ which precludes it from being the $\delta(962)$. Using arguments¹⁷ similar to those made for the $\eta'(958)$, we conclude that the $\eta_N^0\pi^+\pi^-$ mode of the M is mediated by the strong interaction, which implies $G = +1$. The apparent absence of a $\rho^0\gamma$ mode would suggest $C = -1$ for the M .¹⁸

In summary, we have observed an enhancement with mass and width consistent with those of the $\eta'(958)$. All its properties observed in this experiment are similar to those of the $\eta'(958)$ except the $\rho^0\gamma/\pi^+\pi^-\gamma$ decay rate which is significantly different (3.5-4 standard deviations). Unless we are victims of a severe fluctuation in the ρ content of $\eta'(958)$, we have observed a new meson, the $M(953)$. We note in closing that a number of reports in the literature attribute enhancements at about 1 GeV to $\eta'(958) \rightarrow \pi^+\pi^-\gamma$, misfitted as $\pi^+\pi^-\pi^0$. We suggest that a careful study of the ρ^0 content of those effects might prove interesting.

*Work performed under the auspices of the U. S.

Atomic Energy Commission.

¹M. Goldberg *et al.*, Phys. Rev. Lett. **12**, 546 (1964); G. R. Kalbfleisch *et al.*, Phys. Rev. Lett. **12**, 527 (1964); A. Rittenberg, UCRL Report No. UCRL-18863, 1969 (unpublished).

²W. Kienzle *et al.*, Phys. Lett. **19**, 438 (1965); R. Ammar *et al.*, Phys. Rev. Lett. **21**, 1832 (1968); V. Barnes *et al.*, Phys. Rev. Lett. **23**, 610 (1969).

³For a summary of the situation concerning the $H(990)$, see A. Barbaro-Galtieri and P. Söding, in *Proceedings of an Informal Meeting on Experimental Meson Spectroscopy, Philadelphia, 1968*, edited by S. Balalay and A. H. Rosenfeld (Benjamin, New York, 1968), p. 137.

⁴A. Barbaro-Galtieri *et al.*, Rev. Mod. Phys. **42**, 87 (1970); see especially p. 132.

⁵The use of unfitted data avoids mass shifts from incorrectly fitting a γ as a π^0 . After fitting to a π^0 , a $\pi\pi\gamma$ peak at a mass of 0.96 GeV shifts up to about 0.98 GeV.

⁶ θ^* is the angle between the target proton and the outgoing K^-p system in the overall center-of-mass system.

⁷All events that fit the 4C reactions $K^-\pi^-\pi^+p$ and $K^-K^+K^-p$ were removed. Reaction (2) was selected if its χ^2 probability was greater than that of any of the other 1C hypotheses. (These included reactions with a missing π^0 , \bar{K}^0 , n , Λ^0 , and Σ^0 .)

⁸The resolution obtained from an ideogram of a delta function, using mass errors from the kinematic full error matrix, is $\sigma = 8.3 \pm 0.5$ MeV.

⁹The quoted errors have been increased to allow for uncertainties in the background.

¹⁰As is the case with Reaction (3), no evidence for structure in the 955-MeV mass region was observed for events with $MM^2 > 0.01$ GeV².

¹¹This cut encompasses almost all the η' events. A strong $\eta' \rightarrow \eta_N^0 \pi^+ \pi^-$ signal from Reaction (8) (not

shown) is also observed with this selection.

¹²For Reaction (2): M region is 0.945–0.965 GeV; control regions are 0.920–0.940 and 0.970–0.990 GeV. For Reaction (6): η' region is 0.930–0.980 GeV; control regions are 0.905–0.930 and 0.980–1.005 GeV. The $\pi^+\pi^-$ background distributions have been normalized to the central value of the resonance mass using the method employed by Rittenberg (see Ref. 1).

¹³The matrix element used is $\sim k^2 q^2 m^2 \sin^2 \theta$, where $\kappa(q)$ is the γ (π^+) momentum, θ is the angle between the γ and π^+ , and m is the di-pion effective mass (all evaluated in the di-pion rest frame).

¹⁴In order to obtain another quantitative test of the difference between Figs. 1(e) and 1(f) we have used the same matrix element to describe the M decay which best fits the η' Dalitz plot. Taking into account the observed signal to noise in the M region, we have performed a χ^2 test on the $\pi^+\pi^-$ effective-mass spectrum of Fig. 1(e) and obtained a χ^2 probability of less than 10^{-4} . This reflects the 3.5–4 standard deviation difference in the branching ratios.

¹⁵The $\eta_N^0 \pi^+ \pi^-$ and $\pi^+ \pi^- \gamma$ enhancements off K^-p have the same production angular distribution; about 50% of the events have $\cos \theta^* > 0.8$ and the $\cos \theta^* > 0.0$ selection encompasses all the events. Also, both enhancements prefer quasi three-body production.

¹⁶If we assume that the major decay mode of $\delta(962)$ is $\pi\eta$ (as seen in bubble chamber experiments) then we should expect a large $\pi^0 \eta_N^0$ signal in the reaction $K^-p \rightarrow K^-p \pi^0 \eta_N^0$ for $\cos \theta^* > 0.0$ which is not observed.

¹⁷ $G = -1$ would necessitate a large $3\pi/\eta\pi\pi$ branching ratio which is not observed. See Ref. 1 for more details.

¹⁸It should be noted that we cannot completely exclude a $p^0 \gamma$ decay mode since exotic matrix elements can in principle distort the $\pi^+\pi^-$ effective-mass distribution, therefore $C = +1$ cannot be ruled out.

ERRATA

MEASUREMENT OF THE ROTATIONAL CONTRIBUTION TO BRILLOUIN SCATTERING. D. F. Nelson and P. D. Lazay [Phys. Rev. Lett. **25**, 1187 (1970)].

The last two sentences on page 1189 and the first sentence on the following page should read, "The magnitude of the latter is in fine agreement with the predictions of -0.0138 from Eq. (5) for rutile at 5145 \AA . On the basis of this agreement one is justified in choosing the upper signs in Eqs. (9) and (10) as the correct ones. This, in

turn, means $p_{(23)32} = p_{(13)31} = +0.0255$ and $p_{(23)23} = p_{(13)13} = -0.0009 \dots$ "

EXPERIMENTAL OBSERVATION OF NONLINEAR LANDAU DAMPING OF PLASMA WAVES IN A MAGNETIC FIELD. R. P. H. Chang and M. Porkolab [Phys. Rev. Lett. **25**, 1262 (1970)].

The symbol η in Eq. (5) on page 1264 should be ηF , where F is a factor which takes care of the boundary conditions.